Strain coupling between upper mantle and lower crust: natural example from the Běstvina granulite body, Bohemian Massif

Matěj Machek[a,b], Stanislav Ulrich[a,b], Vojtěch Janoušek[b,c]

[a] *Institute of Geophysics AS CR, v.v.i, Boční II/1401, 14131, Prague 4, Czech Republic, mates@ig.cas.cz*
[b] *Institute of Petrology and Structural Geology, Charles University, Albertov 6, 128 43 Prague, Czech Republic*
[c] *Czech Geological Survey, Klárov 3, 118 21 Prague 1, Czech Republic*

published in Journal of Metamorphic Geology 27 (2009) 721-737

Strain patterns within mantle rocks and surrounding coarse-grained felsic granulites from the Kutná Hora Crystalline Complex in the Variscan Bohemian Massif have been studied in order to assess their strain coupling. The studied rock association occurs within low-strain domains surrounded by fine-grained granulite and migmatite. The Doubrava peridotite contains closely spaced and steeply dipping layers of garnet clinopyroxenite, which are parallel to NE–SW-striking, high-temperature (HT) foliation in nearby granulites, while Úhrov peridotite lacks such layering. Spačice eclogite is not associated with peridotite and shows upright folds of alternating coarse- and fine-grained varieties bearing NE–SW striking axial planes. Electron back-scattered diffraction (EBSD) measurements revealed full strain coupling between clinopyroxenites and coarse-grained granulites in the S1 fabric that is superposed on the S_0 fabric preserved in peridotites. The B-type olivine LPO characterizes the S_0 fabric in peridotites and its reworking is strongly controlled by presence of macroscopic clinopyroxenite layering. The S1 in clinopyroxenites and coarse-grained granulites is associated with the LS-type clinopyroxene LPO and prism <c> slip in quartz, respectively. While S_1 fabric in these rock types is accompanied invariably by a sub-vertical stretching lineation, the S_1 fabric developed in reworked Úhrov peridotite is associated with strongly planar axial (010) type of olivine LPO. The peridotites with the S_0 fabric are interpreted to be relicts of a fore-arc mantle wedge hydrated to a various extent above the Saxothuringian subduction zone. The prograde metamorphism recorded in peridotites and eclogites occurred presumably during mantle wedge flow and was reaching UHP conditions. Strain coupling in the S_1 fabric between clinopyroxenites and granulites at Doubrava and upright folding of eclogites at Spačice document a link between tectonic and magmatic processes during orogenic thickening, coeval with intrusions of the arc-related calc-alkaline suites of the Central Bohemian Plutonic Complex (c. 360–345 Ma). Juxtaposition of peridotites and granulites could be explained by a rheological heterogeneity connected to the development of clinopyroxenite layering in the upper mantle and a previously published model of a lithospheric-scale transpressional arc system. It invokes vertical shearing along NE–SW trending, sub-vertical foliations in the upper mantle that could have led to an emplacement of mantle bodies into the granulitized, orogenic root in the sub-arc region. Clearly, such a transpressional arc system could represent an important pathway for an emplacement of deep-seated rocks in the orogenic lower crust.

1 Introduction

The degree of coupling (or decoupling) between the lithospheric layers during the continental deformation has significant implications for all aspects of modern or ancient orogenesis. Zones of strain coupling link rheological domains vertically in the lithosphere, such zones fundamentally differ from the basal detachment zones. It is because they provide kinematic compatibility and attachment between domains that have accommodated strain in different ways (Molnar, 1992; Grocott et al., 2004; Tikoff et al., 2004). Although popular concept of strain decoupling at the crust–mantle interface may certainly be applicable in some case, a number of geological and geophysical observations (e.g. Vauchez & Barruol, 1996; Barruol, 1997) clearly demonstrate the strain coupling, often enhanced by the presence of partially molten rocks (De Saint Blanquat et al., 1998; Vigneresse & Burg, 2004).

Fragments of mantle rocks are common within the high-grade crustal units of the European Phanerozoic orogenic belts. They are represented by spinel or garnet peridotite, websterite, dunite, clino- or orthopyroxenite, and eclogite. All of these rock types have been traditionally subject to mainly geochemical and petrophysical studies aimed at explaining their origin, petrology, age, and seismic properties. In addition, their interactions with other rock types and evolution during plate tectonic processes were also investigated. These so-called "orogenic peridotites" form tectonic lenses of hundreds of meters to kilometers long within medium- to high-grade metamorphic crustal rocks (e.g. Medaris et al., 1990; Altherr & Kalt, 1996). They frequently record very-high-pressure conditions (>3.0 GPa). Unfortunately, models of emplacement into crustal rocks are often based solely on geochemical and petrological arguments, without assessment of the internal strain fabric of the mantle rocks themselves (e.g. Altherr & Kalt, 1996; Medaris et al., 2005).

In the Variscan Bohemian Massif, garnet and spinel peridotites with associated eclogite and pyroxenite bodies occur enclosed in granulites of the Gföhl unit, which represents the most metamorphosed part of the internal orogenic zone, called the Moldanubian domain (Mísař et al., 1983; Franke, 2000). Internal strain fabric study of these mantle rocks and granulites, together with the petrology and geochemistry, could provide vital constraints on the nature and extent of the crust–mantle interaction during the Late Paleozoic collision in European Variscan orogeny. This orogeny in the Bohemian Massif has been explained as a multi-stage Devonian-to-Carboniferous collision of continental fragments. It involved high-grade metamorphism and reworking of continental crust in the orogenic root (Schulmann et al., 2009) decoupled from the deformation in the upper mantle (Schulmann et al., 2005). Seismic anisotropy of a mantle lithosphere below the Bohemian Massif revealed different fabrics underlying the main Variscan crustal tectonic domains. It has been interpreted as a pre-Variscan frozen-in fabric supporting the idea of strain decoupling during the Variscan orogeny (Babuška & Plomerová, 2006). Geochemical and petrological studies of mantle rocks from HT crustal rock assemblages led to the conclusion that they originated as a Late Devonian volcanic arc and an associated back-arc basin that was telescoped and imbricated during the Carboniferous collision (Medaris et al., 1995). To date, however, analysis of strain features in orogenic peridotites has never been compared with surrounding high-grade crustal rocks (granulites) with an intention to assess the degree of strain coupling and to discuss emplacement mechanisms. This is mainly due to the strong serpentinization of peridotites that renders field measurements of strain features impossible.

In this work, the internal strain fabric of peridotites, clinopyroxenites, and eclogites enclosed in the granulites of the Běstvina granulite body of the Gföhl unit is established using measurements of the lattice preferred orientation of the main rock-forming minerals and comparison with surrounding granulites. All data are discussed in the context of the P-T estimates and geochemical analyses presented elsewhere. The main goals are to assess the degree of strain coupling between mantle fragments and the lower crust and to establish a feasible mechanism for emplacement of the studied mantle peridotites into granulites.

2 Geological setting

The Variscan orogeny occurred due to Devonian-to-Carboniferous convergence of peri-Gondwanan crustal segments (the Saxothuringian, Teplá-Barrandian, Moldanubian and Brunia domains; Dudek, 1980; Franke, 2000) (Fig. 1) to the south and Baltica to the north (Ziegler, 1986; Tait et al., 1996). Based on geochronology, petrology, and detailed structural works, Schulmann et al. (2009) concluded that Variscan orogeny in the Bohemian Massif started in the middle Devonian by subduction of the Saxothuringian Ocean below the Teplá-Barrandian (fore-arc) triggering back-arc spreading in the Moldanubian domain. Further convergence of Brunia toward the Moldanubian domain in the east and closure of the Saxothuringian Ocean followed by a deep subduction of the Saxothuringian continental crust (O'Brien, 2000; Janoušek et al., 2004a; Konopásek & Schulmann, 2005; Janoušek & Holub, 2007) in the west led to the formation of an orogenic root from the Moldanubian domain that had been rheologically softened in the back-arc position (Schulmann et al., 2009). This episode was associated with intrusion of the arc-related, c. 360–345 Ma old, normal- to high-K calc-alkaline magmatic suites of the Central Bohemian Plutonic Complex (e.g. Košler et al., 1993; Holub et al., 1997; Janoušek et al., 2000; 2004a,b; submitted) and transpressional deformation along the magmatic arc (Žák et al. 2005a). Orogeny continued by the extrusion of high-grade rocks from the orogenic root to the mid-crustal levels (Žák et al., 2005a; Schulmann et al., 2008) and voluminous intrusions of (ultra-) potassic rocks and anatectic (S-type) granites (e.g. Dallmeyer et al., 1995; Timmerman, 2008).

The studied bodies of garnet peridotite and eclogite occur in the Běstvina Formation of the Kutná Hora Crystalline Complex (KHCC) that is located at the northern margin of the Moldanubian domain (Suess, 1926). Based on lithologies and metamorphic conditions, the Kutná Hora Complex belongs to a high-grade Gföhl unit (Synek & Oliveriová, 1993). From the plate-tectonic point of view, it occurs on the back-arc side of the magmatic arc (Central Bohemian Plutonic Complex). In the KHCC, three major units were defined that are thought have resulted from progressive nappe stacking and metamorphic inversion during Variscan orogeny (Synek & Oliveriová, 1993). The base

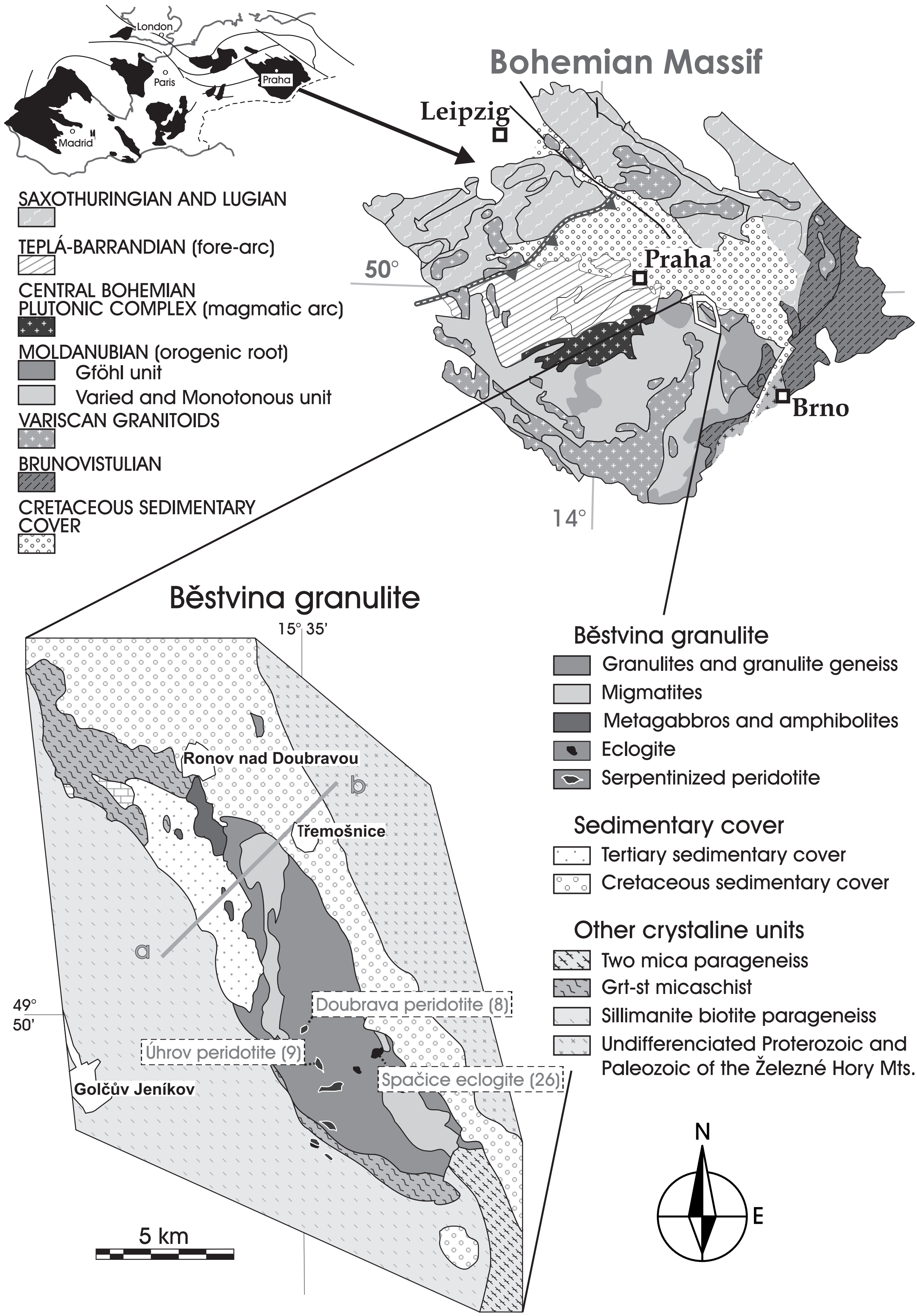

Fig. 1. *(a) Simplified geological map of the Bohemian Massif with major tectonic units (after Franke, 2000) and geological map of studied area (Běstvina granulite) with marked position of structural cross-section (Fig. 2b) and mantle rock localities (name and number for each of the localities as used in text).*

of the nappe pile consists of meta-sedimentary sequences of the Monotonous unit, tectonically the lowermost, medium-grade part of the Moldanubian zone. In the hanging wall, the Micaschist zone is built by muscovite–biotite-bearing micaschists with intercalations of diopsidic amphibolite. The Micaschist zone is overlain by partially molten and strongly sheared orthogneiss (the Kouřim nappe) in the west and metagabbros (of the Svatý Kříž Massif; Munchi, 1978, 1981; Holub & Munchi, 1984) in the east. The tectonically uppermost part, being assigned to the Gföhl unit, comprises bodies of high-grade granulites enclosing eclogites and garnet peridotites. This unit was subdivided into Běstvina, Malín, and Plaňany bodies based on geographical position and metamorphic evolution (Synek & Oliveriová, 1993).

The studied Běstvina granulite body consists mainly of retrogressed felsic granulites, biotite gneisses, migmatites, and several small, isolated bodies of peridotite and eclogite (Pouba, et al. 1987; Synek & Oliveriová, 1993) (Fig. 1). Vrána et al. (2005) subdivided felsic rocks of the so-called Běstvina Formation, based on geochemical and petrological data, into metamorphosed greywacke and two types of metaigneous granulite/migmatitic gneiss. They proved eclogite-facies equilibration conditions for granulite and meta-greywacke (T = 800–920 °C, P = 1.8–2.2 GPa), as well as a significantly lower degree of metamorphism for the migmatitic gneiss (T = 670 °C, P = 1.4 GPa).

Three bodies of mantle rocks have been chosen for the current work. Úhrov peridotite (locality no. 9) and Spačice eclogite (locality no. 26) have already been studied from the petrological and geochemical points of view (Medaris et al., 1995, 2006a,b; Faryad, 2009). Geochemical studies show that Úhrov peridotite originated from a subcontinental lithosphere; garnet pyroxenite and eclogite enclosed in the peridotite are thought to represent high-pressure crystal cumulates from melts that migrated through the lithospheric mantle (Medaris et al., 1995 Medaris et al., 2005).

The eclogite enclosed in the granulite at Spačice contains an assemblage of garnet with a prograde zoning, omphacite, quartz, rutile and plagioclase that yields estimated peak metamorphic conditions of 1.8–2.0 GPa and 835–935 °C, which is comparable to those determined from the host felsic granulite (Medaris et al., 2006b). However, Faryad (2009) argued that plagioclase belongs to the retrograde assemblage and calculated that maximum P-T conditions could have been 3.4 GPa and 910 °C.

Additionally, a newly discovered body called the Doubrava peridotite (locality no. 8) is described in this work because it contains a well-exposed assemblage of peridotite, eclogite and clinopyroxenite in an exceptional structural relationship. Calculated P-T conditions for Úhrov and Doubrava peridotite document prograde evolution from spinel to a garnet stability field up to a peak of 4.5 GPa/950 °C (Medaris et al., 1995; Faryad, 2009). Maximum P-T conditions of 3.4 GPa/960 °C were calculated for eclogites as well as clinopyroxenite layers enclosed in peridotites (Faryad, 2009).

3 Structure

Two deformation fabrics have been recognized within the Běstvina granulite. The earlier S_1 fabric occurs within the low-strain domains surrounded by regionally developed penetrative S_2 fabric. The S_1 fabric in felsic granulites and granulite gneisses shows coarse-grained, high-temperature foliation steeply dipping to the SE or NW (Fig. 2) and is usually preserved in the vicinity of peridotite and eclogite bodies. The Doubrava peridotite (locality 8) is an approximately 40 m wide, intensely serpentinized body bearing no signs of a foliation pattern. There are small lenses of garnet-rich eclogite enclosed within, but they have an unclear structural relationship to the peridotites. A main

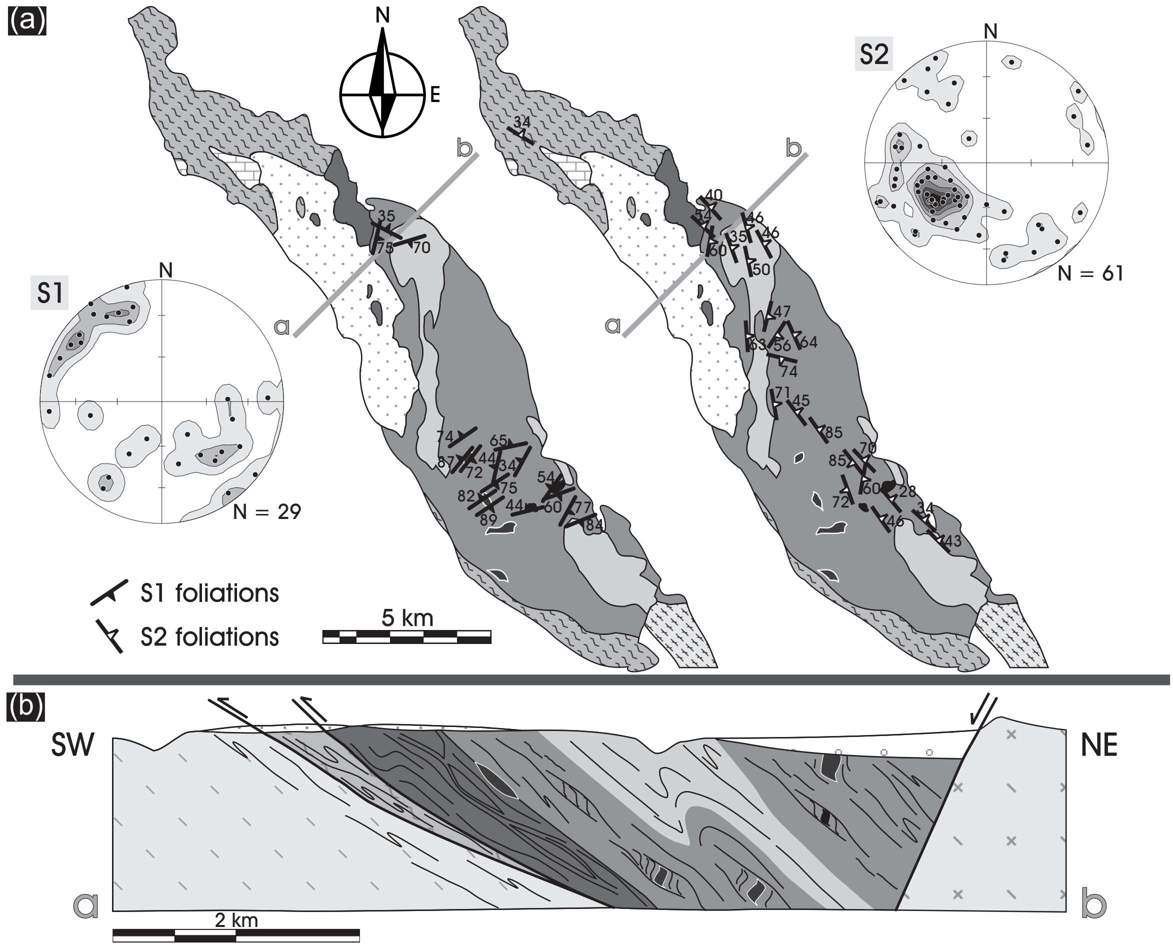

Fig. 2. *Structural maps of Běstvina granulite with stereographic projections, S1 fabric on the left and S2 fabric on the right. (b) Simplified structural cross section of Běstvina granulite. Legend for rock types is given in Figure 1.*

macrostructural feature is the occurrence of closely spaced, steeply dipping olivine and garnet clinopyroxenite layers (Fig. 3a), which are up to 40 cm wide and mostly parallel to S_1 foliation in granulite. Only locally are they bent around the eclogite lenses. The Úhrov peridotite (locality 9) forms a ∼ 100 m wide body in granulite gneisses, which itself encloses small lenses of garnet-rich eclogites. It is less serpentinized than the Doubrava peridotite and shows a local alignment of garnet grains defining S_1 fabric. The Spačice eclogite (locality no.26) forms a sigmoidal body ∼ 60 m long, which occurs within granulite gneiss and is not associated with any peridotite at all. The eclogite exhibits alternating coarse- and fine-grained variety, which are tightly to isoclinally folded (Fig. 3b), with axial planes parallel to the S_1 foliation. The penetrative S_2 fabric occurs in medium-grained granulite gneisses or migmatites and shows homogeneous penetrative foliation lacking stretching lineation and kinematic indicators. The S_2 foliation dips generally to the ENE at medium to high angles (Fig. 2). Occasionally, a transposition of the S_1 into the S_2 foliation by symmetrical folds is preserved within the S_2 fabric, showing parallelism between folds axial planes and the S_2 foliation. .

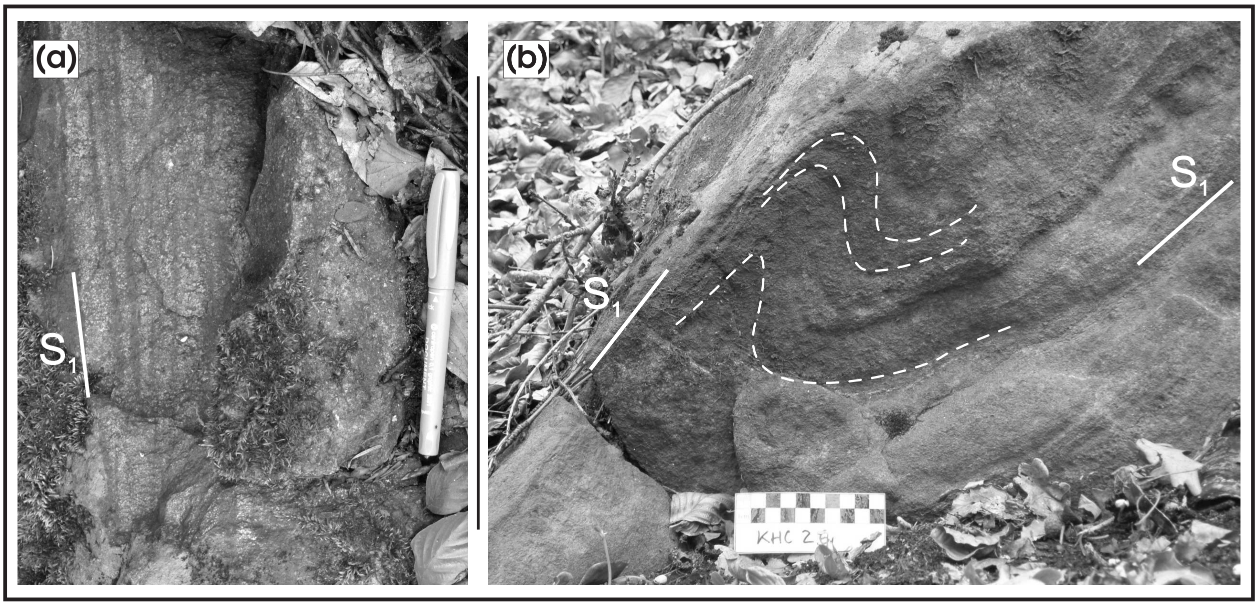

Fig. 3. *Field photographs. (a) Clinopyroxenite layering (S1) exposed at Doubrava. (b) Folded eclogite at Spačice.*

4 Microstructure and Petrography

The microstructure has been studied within the low-strain domains in all rock types (Fig. 4). Thin sections were cut perpendicular to the foliation and parallel to either dip direction (mantle rocks) or stretching lineation (granulites). In the case of mantle rocks, new thin sections have been made according to the results of the LPO measurements of both pyroxenes; the aim was to observe XZ sections of the finite-strain ellipsoid. The sections were photographed, and grain boundaries traced manually from the photomicrographs. Serpentinization in all studied thin sections occurred statically, and thus the original microstructure could be reconstructed using a set of photomicrographs taken in plain and crossed polarized light as well as reflected light. The aim was to assess the original extent of individual grains. The grain boundaries were drawn in the ESRI ArcView© 3.3 GIS environment, and the resulting shape files were processed using MATLAB™ PolyLX Toolbox (Lexa et al., 2005) to obtain average grain size and degree of serpentinization. The average grain size is given by the Feret diameter ($F = 2\sqrt{(A/\pi)}$, where A is the grain area).

4.1 Doubrava peridotite body

Peridotite (samples: 8-05-v3, 8-05-v8, 8-05-v11, 8-07-c) in the Doubrava body (Fig. 4a) consists of relic olivine (Fo = 0.90–0.92), clinopyroxene (Di = 0.70–0.73), orthopyroxene (X_{Mg} = 0.91–0.92), garnet (Py = 66–78), spinel, and amphibole. Dark red, Cr-rich spinel (spinel I) ($X_{Al} = Al/(Cr + Al + Fe^{3+}) = 0.38$) forms isolated grains in the matrix and occurs also as inclusions in both garnet and clinopyroxene. Yellow–red spinel (spinel II) with relatively low Cr content (X_{Al} = 0.55–0.66) is present in the matrix and in the symplectites around garnet. Detailed textural and compositional relations of minerals in the peridotite were described by Faryad (2009). Serpentinization extends to 56 % of the rock volume and is demonstrated by the appearance of antigorite crystals. They grow

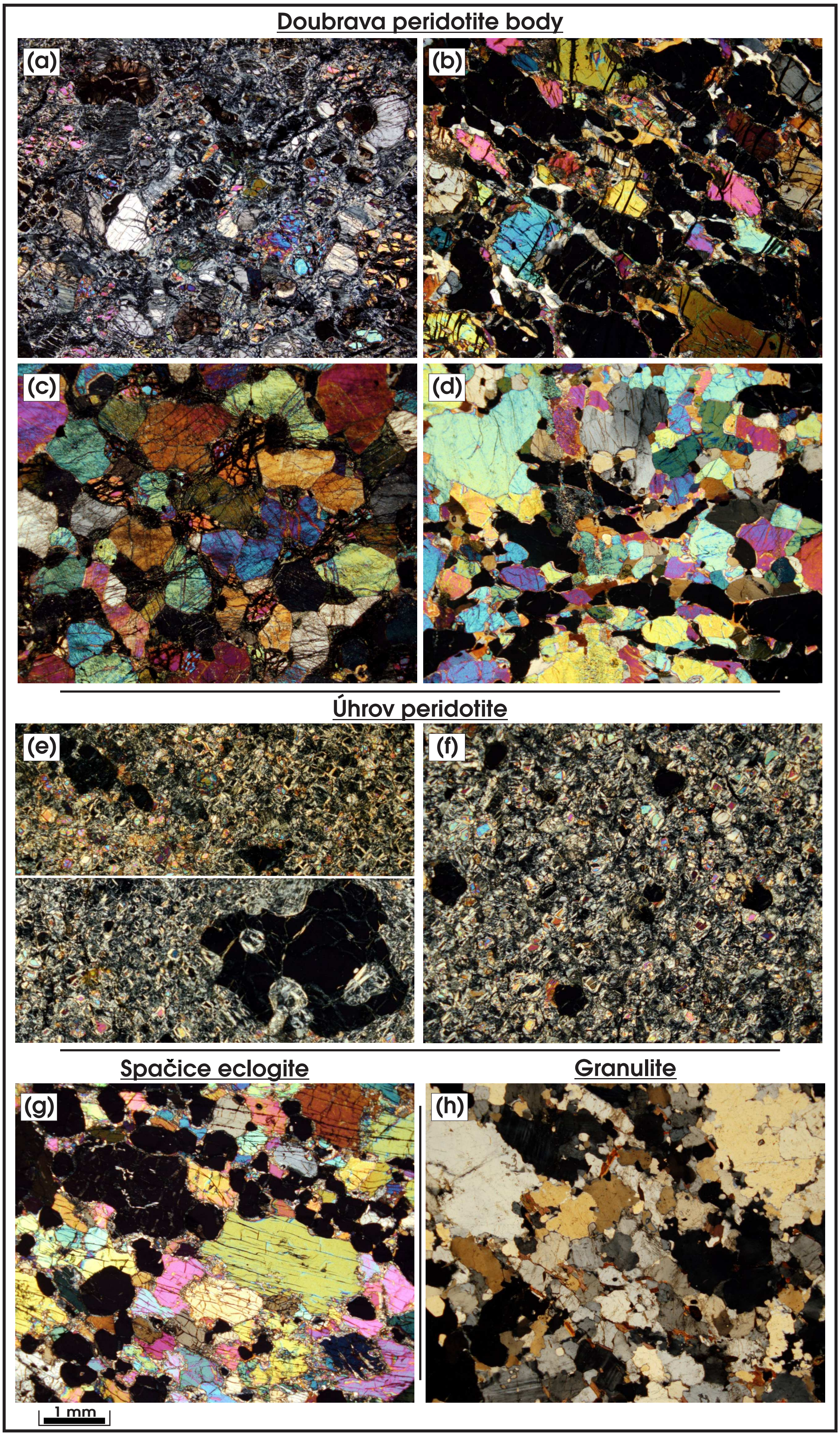

Fig. 4. Photomicrographs taken in cross-polarized light show microstructures of typical rock types at Doubrava (locality 8): (a) peridotite, (b) eclogite, (c) olivine clinopyroxenite, (d) garnet clinopyroxenite, (h) granulite; Úhrov (locality 9): (e) coarse-grained garnet peridotite, (f) fine-grained garnet peridotite; Spačice (locality 26): (g) eclogite. Scale bar at the bottom of the figure belongs to all photographs.

first at the expense of olivine and/or along cleavage of orthopyroxene; fnally they grow topotactically and replace whole grains. Locally, chrysotile and carbonate veins with thin and short bands of magnetite are present in highly serpentinized domains. The original microstructure was probably coarse grained, equigranular interlobate without signs of dynamic recrystallization. Mean Feret diameters of olivine, clinopyroxene, and orthopyroxene grains show similar values close to 0.45 mm.

Eclogite (samples: 8-05-n, 8-06-ec, 8-06-1b) in Doubrava peridotite body (Fig. 4b) consists mainly of primary omphacite, garnet, apatite, and rutile. Original omphacite is broken down to a symplectite of diopside, plagioclase, and amphibole following grain boundaries and cracks in the host crystals. The primary equilibrated microstructure was coarse grained with microscopically clearly visible foliation formed by compositional banding and elongation of omphacite, garnet, and apatite. Omphacite and garnet grain sizes range from 0.1 mm to 3.1 mm and from 0.15 mm to 1.2 mm, with mean Feret diameters of 0.4 and 0.5 mm, respectively. Effects of dynamic recrystallization of primary grains have not been observed, and there is also no sign of deformation of symplectites or secondary minerals.

Two varieties of pyroxenite are present in the Doubrava peridotite body. The first type (Fig. 4c) (samples: 8-05-v2, 8-05-v9, 8-06-4b) is enclosed in peridotite and consists of a dominant diopside ($Di_{0.69\text{-}0.70}$), with subordinate olivine (Fo = 0.82–0.87), garnet (Py = 56–65), dark red spinel I, pyrite, and rare orthopyroxene with secondary amphibole that sporadically forms rims around garnet grains. The pyroxenite is characterized by a relatively high volume of olivine (up to 28 %) and subordinate garnet (less than 2 %). Diopsides are coarse (grain size between 0.1 and 1.7 mm, with mean Feret diameter of 0.6 mm) and show straight grain boundaries, often forming 120° triple junctions between grains. Olivine shows smaller grain sizes (between 0.07 and 1.0 mm, with mean Feret diameter of 0.4 mm) and anhedral grain shapes, and it is partly serpentinized. Relic garnet is mostly replaced by pyroxene and spinel symplectites, although some garnet grains contain inclusions of clinopyroxene and spinel. Most spinel grains occur interstitially between adjacent diopsides, but some form inclusions in clinopyroxenes.

The second pyroxenite type (Fig. 4d) (samples: 8-2a, 8-3a) occurs next to one eclogite lens and is characterized by abundant garnet (~20 %), high contents of amphibole (~10 %) and an absence of olivine relics. Pyroxene is large (grain size between 0.1 and 1.8 mm) with straight grain boundaries and triple-point junctions between grains. Garnet is rounded or elongated with 0.4 mm mean grain size. Amphibole having anhedral shapes concentrates around garnets and replaces clinopyroxenes.

A **granulite** (sample khc8e) in the vicinity of the Doubrava peridotite displays coarse-grained, inequigranular–interlobate microstructure (Fig. 4h) built by plagioclase, quartz, garnet, biotite, K-feldspar, rutile, and kyanite. Foliation is defined by elongation of large plagioclase and quartz grains. High-pressure mineral assemblage with kyanite, Ca-rich garnet ($Grs_{41}Py_{13}Alm_{45}Sps_1$), ternary feldspar, and accessory rutile (Nahodilová et al., 2008) disappears, and the amount of plagioclase, K-feldspar, and biotite increase. This retrogression of the HP granulite is accompanied by coarsening and formation of relatively Ca-poor garnet (Grs_{22} Py_{22} Alm_{55} Sps_1).

4.2 Úhrov peridotite body

Two microstructural varieties have been observed in the Úhrov peridotite body (Fig. 4e,f). Both consist of olivine, clinopyroxene, orthopyroxene, garnet, and spinel and show interlobate microstructure that lacks features induced by dynamic recrystallization. In both types, individual garnet grains and thin (some 2 mm) and discontinuous pyroxenite bands occasionally align along S_1 foliation. In the sample khc9a, a large orthopyroxene grain with clinopyroxene and garnet exsolutions has been observed within the pyroxenite band. The main difference between both microstructural types is in the garnet grain size. In the first type (samples: khc9 and khc9a), the average grain size of olivine and pyroxenes is about 0.2 mm ranging up to 0.4 and 0.5 mm, respectively, while the size of garnet grains reaches 4 mm. The garnet grains may contain inclusions of serpentinized olivine, clinopyroxene, and dark red spinel. The second type (samples: khc9b-2, 9-07a) is slightly coarser, with grain sizes of olivine and pyroxenes up to 0.9 and 0.6 mm, respectively, and an average garnet grain size of 0.4 mm. Minerals in both microstructural types show compositions similar to those measured in Doubrava garnet peridotite, except that they have slightly higher X_{Mg} contents in the garnet (Faryad, 2009).

4.3 Spačice eclogite

Eclogites (Fig. 4g) (samples: 26-05-g, 26-05-v3) contain omphacite, garnet, zoisite, kyanite, apatite, and rutile. During retrogression, they have formed symplectites and coronas around garnets, consisting of diopsidic clinopyroxene, plagioclase, spinel, and amphibole. In one case, a zoisite-bearing variety of eclogite was found. Zoisite forms short columnar grains in almost monomineral bands (3–5 mm thick) with small amounts of omphacite, garnet, and pseudomorphs after kyanite. Plagioclase replaces zoisite along grain boundaries and at contacts with omphacite and garnet. Based on textural relations, zoisite seems to be a stable phase in the HP assemblage. Foliation is defined by compositional banding as well as elongation of omphacite, garnet, and zoisite. There are two microstructural varieties that differ in grain size and form bands parallel to the S_1 fabric, alternating on both the hand specimen and the thin-section scale. Omphacite and garnet grain sizes range from 0.1 mm to 1.9 mm and from 0.2 mm to 0.9 mm, respectively. Fine-grained varieties contain neither porphyroclasts nor signs of dynamic recrystallization of primary grains. The retrogression took place in a static environment because there is no record of deformation of symplectites or secondary minerals.

5 Lattice preferred orientations

A numerical modeling of olivine as well as clinopyroxene LPO development revealed that the symmetry of LPO and the activity of different slip systems may change due to a deformation regime (e.g., pure shear, simple shear, transpression, and transtension; Tommasi et al., 1999; Bascou et al., 2002). A database of olivine LPO from naturally deformed peridotites has shown [100](010) (Type A), [100]{0kl} (Type D) and axial [010] (Type AG) patterns (Fig. 5) and corresponding slip systems as the most common in different geotectonic environments,.The [001] Burgers vector may also become active at lower temperatures (Ben Ismaïl & Mainprice, 1998; Tommasi et al., 2000). Mineral physics studies showed that the activity of olivine slip systems is sensitive to both pressure (Mainprice et al., 2005) and water content (Chopra et al., 1984; Mackwell et al., 1985). It was argued that the LPO of olivine can be modified under water-rich conditions based on the flow stress (Types B, C, and E) (e.g. Bystricky, et al., 2000; Zhang et al., 2000; Jung & Karato, 2001; Katayama et al., 2004) (Fig. 5) mainly in the mantle wedge above a subducted plate (Kneller et al., 2007). The most commonly observed texture of clinopyroxenes (e.g. Godard & Van Roermund, 1995; Mauler et al.,

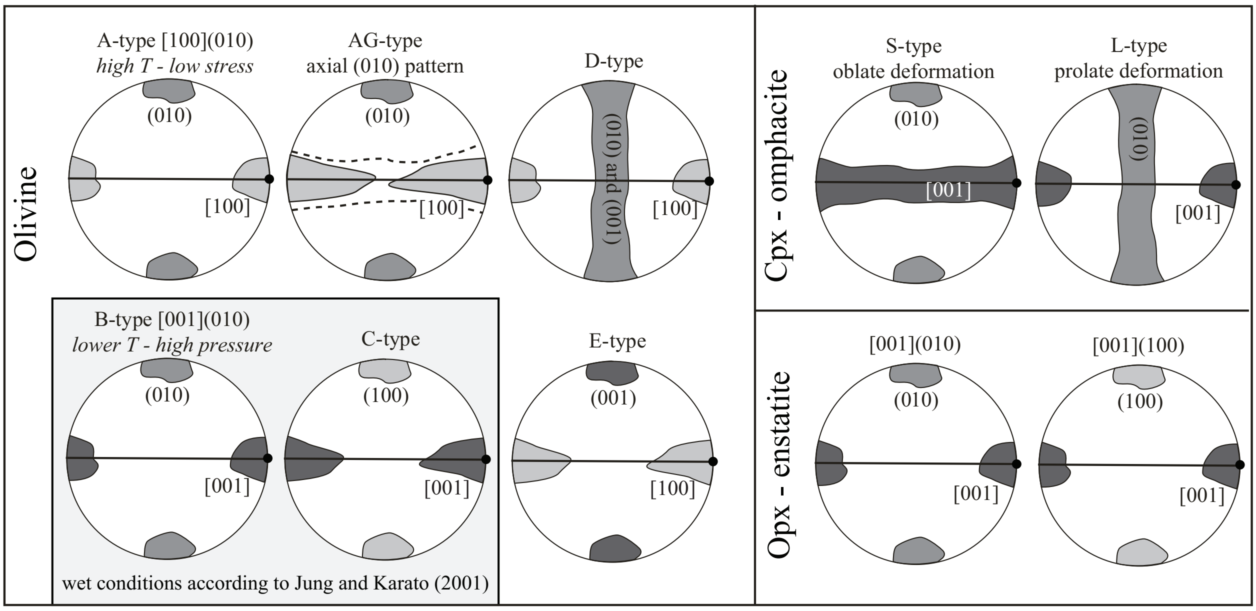

Fig. 5. *Idealized pole figures summarizing typical olivine, clinopyroxene and orthopyroxene LPO patterns observed in mantle rocks. Horizontal line is orientation of foliation with lineation (black circle).*

2001; Bascou et al., 2002) corresponds to activity of ½ < 110 > {1 0}, [001]{110} and [001](100) slip systems. Clinopyroxene LPO measured in naturally deformed eclogites showed that it is a combination of two textural end members of LPO called L type and S type (Fig. 5) (Helmstaedt et al., 1972). The most common LS type shows (010) poles normal to the foliation and [001] axes defining lineation, and this is supported by numerical modeling (Bascou et al., 2002). In eclogites, clinopyroxene LPO can be used as a quantitative indicator of strain symmetry calculating the LS index. It has a value of one for the end-member L-type, zero for the end-member S-type and intermediate values for LS-types (Ulrich & Mainprice, 2005). Naturally deformed orthopyroxenes show a strong tendency toward alignment of [001] axes parallel to stretching lineation and either the (100) or (010) planes being parallel to foliation (Fig. 5) (e.g. Etheridge, 1975; Ross & Nielsen, 1978; Sawaguchi & Ichii, 2003). It is therefore very likely that dominant dislocation glide in naturally deformed orthopyroxene will operate on (010)[001] and (100)[001] slip systems, respectively.

5.1 Methods

Lattice preferred orientation (LPO) of olivine, clinopyroxene, orthopyroxene, plagioclase, and quartz grains was measured using the electron back-scattered diffraction (EBSD) method. The EBSD patterns have been obtained using professional software and a CCD camera (Oxford Instruments) attached to the scanning electron microscope CAMSCAN 4 at the Institute of Petrology and Structural Geology, Charles University in Prague. Diffraction patterns were acquired using an acceleration voltage of 20 kV, a 39 mm working distance, and ~5 nA beam current. The whole procedure (pattern acquisition, image freezing, band detection, indexing, and result backup) was carried out on the studied sample manually due to its large size and the strong serpentinization of the original grains. Thus, each individual grain is represented only by a single orientation measurement. In the case of granulites and clinopyroxenites, well-defined

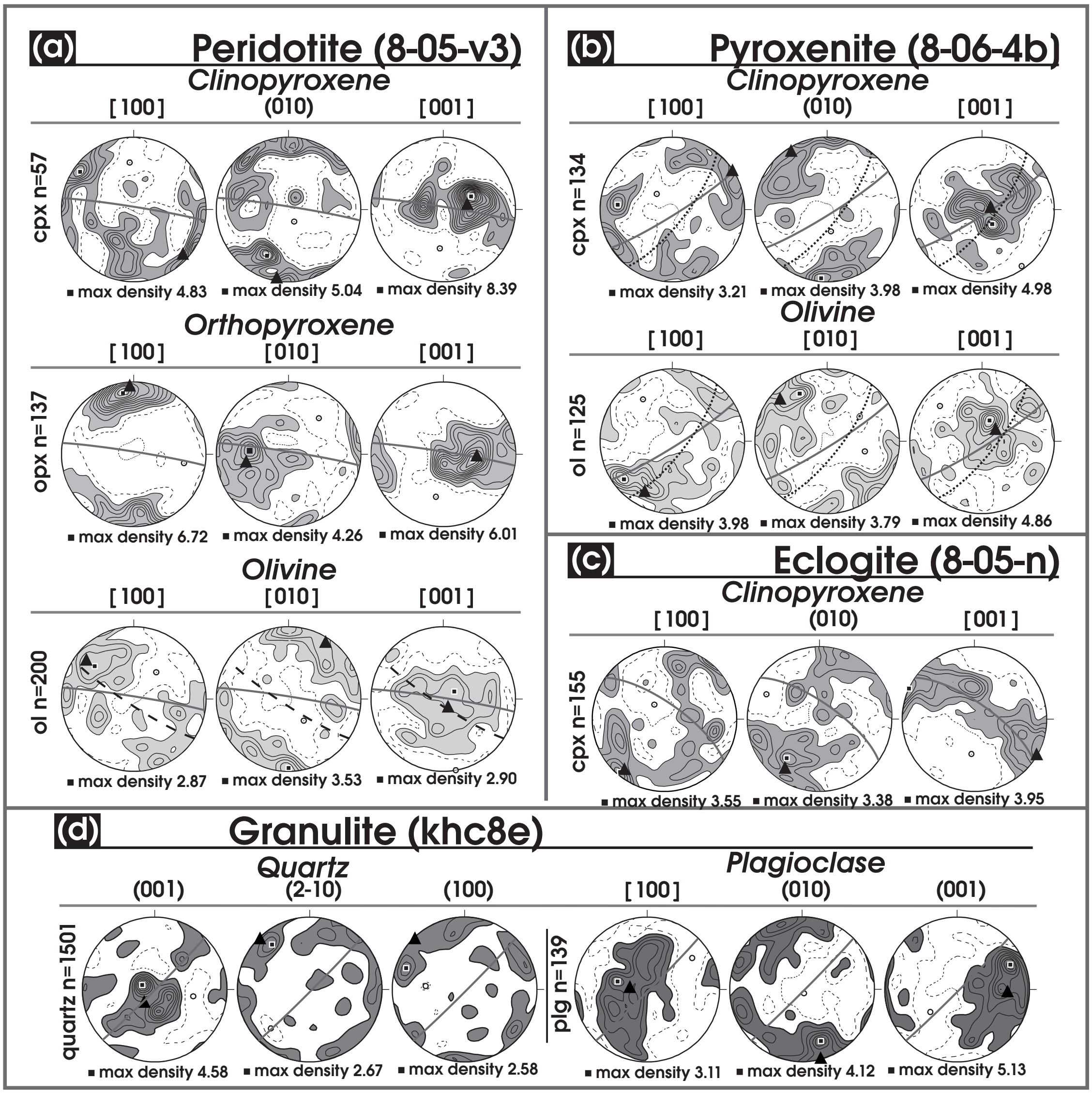

Fig. 6. *Lattice preferred orientations (LPO) of main rock-forming minerals in all rock types at Doubrava peridotite body (locality 8), presented in a lower hemisphere equal area projection. Pole figures are in geographic coordinates. Contour level is 0.5 multiples of uniform distribution. Areas of pole figures above contour one are in grey color, Black triangle marks position of the longest eigenvector obtained by analysis of the normalized orientation tensor for principal crystallographic directions and n is a number of measured grains. Full line represents foliation determined according to orientation of the LS type LPO pattern in clinopyroxene. (a) LPOs of clinopyroxene, olivine, and orthopyroxene in peridotite; dashed line represents plane perpendicular to the longest eigenvector of [010] olivine pole figure. (b) LPOs of clinopyroxene and olivine in clinopyroxenite; dotted line represents orientation of clinopyroxenite layers in the field. (c) LPO of clinopyroxene in eclogite. (d) LPOs of quartz and plagioclase in granulite.*

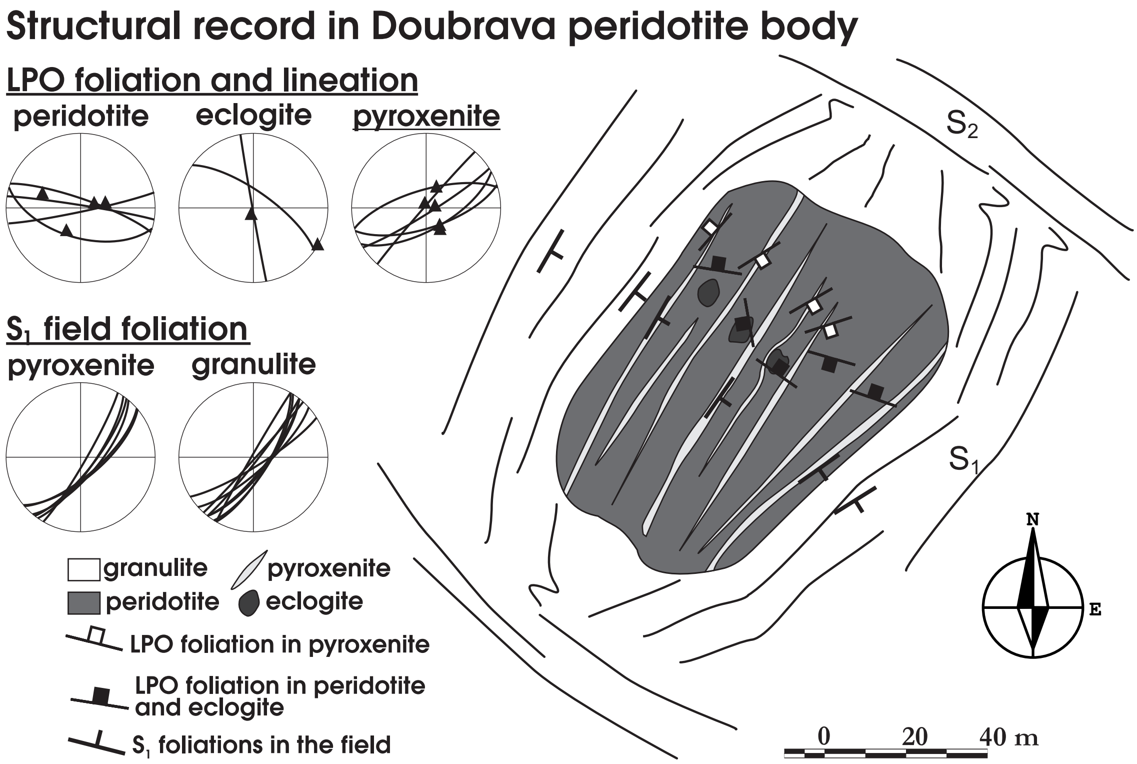

Fig. 7. *Structural record in Doubrava peridotite body. Schematic map view and stereographic projections of field structure and LPO foliations.*

foliation and orientation of pyroxenite layers seen in the field facilitated identification of dominant slip systems in measured rock-forming minerals, and consequently also the estimation of principal directions of finite-strain ellipsoid. However, especially in the case of strongly serpentinized peridotites, the LPO of olivine was compared to the LPOs of clinopyroxene as well as orthopyroxene in every measured sample. Orientations of foliation and lineation in the peridotite sample have been determined according to the geometrical fit between the LS-type LPO pattern in clinopyroxene, the most common slip systems (100)[001] and (010)[001] in orthopyroxene, and several possible slip systems in olivine as it was outlined above.

The eigenvector analysis of the normalized orientation tensor has been carried out for the principal crystallographic directions and plotting of the longest eigenvectors (λ_1) to individual pole diagrams using the Unicef careware software package developed by D. Mainprice (2005). In clinopyroxenites and eclogites, the clinopyroxene LPO has been used also for quantification of strain symmetry using the LS index (Ulrich & Mainprice, 2005). Consequently, the measured data and eigenvector positions have been rotated into geographic coordinates.

5.2 Results

In the **Doubrava peridotite**, the LPOs of both pyroxenes determine steep, E–W striking foliations with sub-vertical to steeply plunging lineation (Fig. 6a, 7; Table 1; supplementary Fig. S1). The olivine LPOs show usually good coincidence between its (010)ol planes with (010)cpx and (100)opx. and parallelism of [001] axes in all minerals. This is consistent with a dominant activity of the (010)[001] slip system in olivine

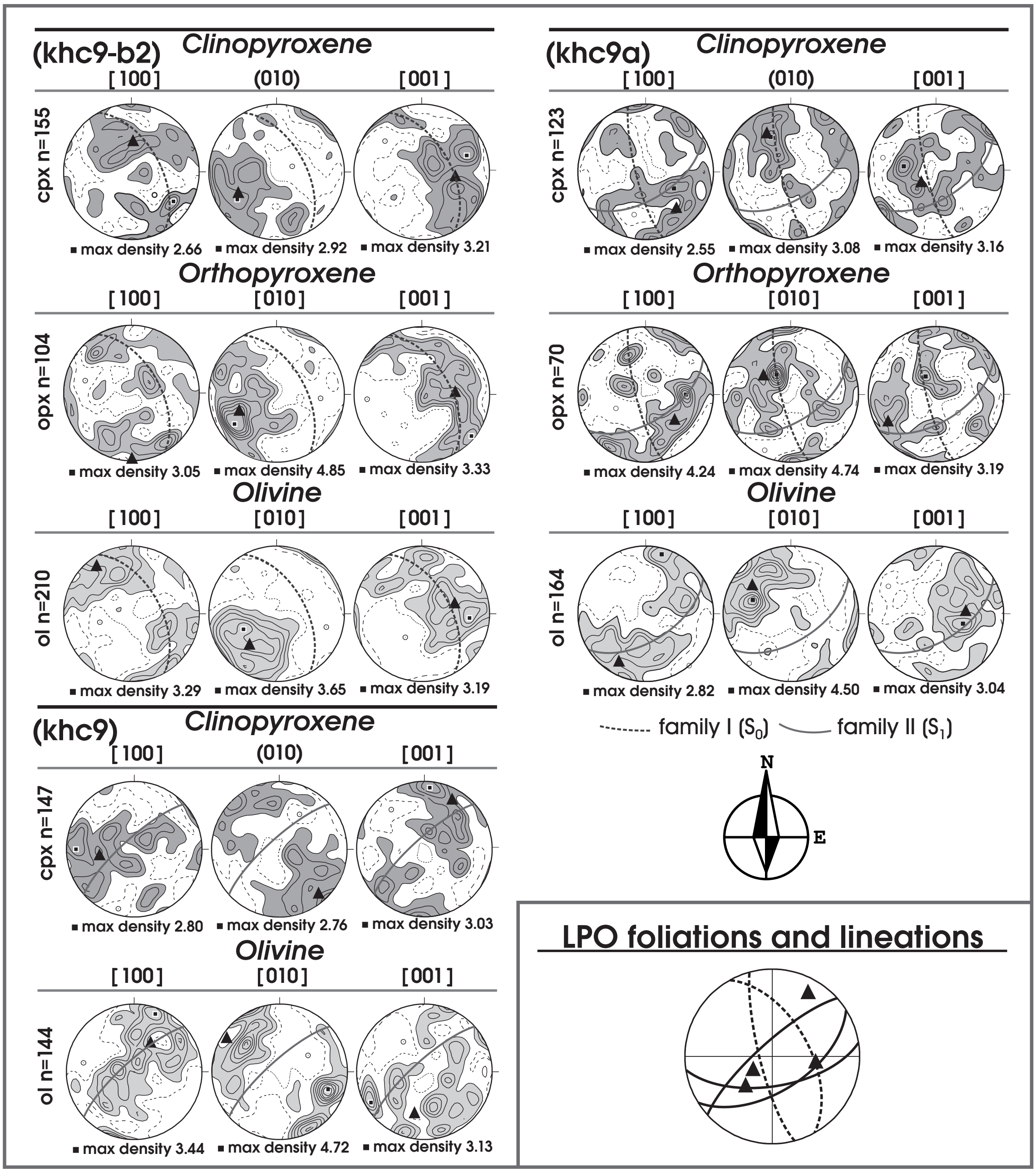

Fig. 8. *Lattice preferred orientations (LPO) of main rock-forming minerals in peridotite at Úhrov (locality 9). Pole figure was constructed, and symbols used, in the same way as in Fig. 6. The dashed line in the clinopyroxene and orthopyroxene pole figures for sample khc9a represents the orientation of the LS-type LPO pattern of family I of clinopyroxene grains; the solid line represents the orientation of the LS-type LPO pattern of family II of clinopyroxene grains in sample khc9a.*

(B type after Jung & Karato, 2001). Other samples show also axial (010) pattern (AG type) of olivine LPO or less clear olivine LPO with the highest concentration of main crystallographic axes oriented obliquely to foliation and lineation defined by both pyroxenes.

All samples of both **pyroxenite types** show subvertical foliation trending NE–SW with subvertical lineation (Fig. 6b, 7; Table 1; Fig. S1). There is systematic, ~ 10º misfit between pyroxenite layering measured in the field and foliation obtained from the LPO analysis. The calculated LS index for clinopyroxene LPO attains small values of 0.32–0.45 in both olivine-free samples as well as in one olivine-bearing sample (8-06-4b). On the other hand, the two other olivine-bearing samples, 8-05-v2 and 8-05-v9, yield much higher LS indexes of 0.73 and 0.61 (Table 1). Better preserved olivine in one sample (8-06-4b) yielded (010) planes parallel to the foliation and [001] directions parallel to the orientation of the [001] axes in clinopyroxenes. This suggests activity of the (010)[001] slip system.

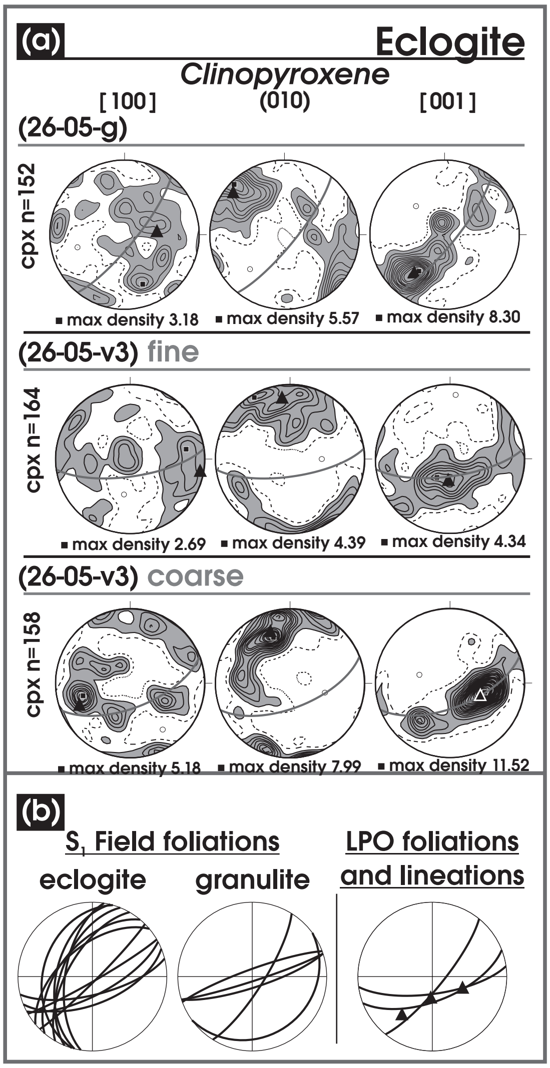

Fig. 9. *Lattice preferred orientations (LPO) of clinopyroxene in eclogite at Spačice (26) (a). Pole figure was constructed, and symbols used, in the same way as in Fig. 6. (b) Structural record in Spačice eclogite body, stereographic projections of field structure and LPO foliations.*

Clinopyroxene LPO in **eclogites** shows pattern close to the S-type that defines strong subvertical NW–SE trending foliations (Fig. 6c; Table 1; Fig. S1). The calculated LS index in four measured samples ranges between 0.36 and 0.46.

Quartz LPO in the coarse-grained **granulite** (Fig. 6d) is characterized by strong sub-vertical maxima of c-axes parallel to the NE–SW trending S1 foliation and m-axes maxima perpendicular to the foliation. Plagioclase LPO exhibits maxima of [100] axes close to vertical orientation, as do the quartz c-axis maxima. The observed LPO pattern of plagioclase, together with the parallel orientation of the c-axes in quartz and [100] axes in plagioclase, suggest activity of (010)[100] and (001)[100] slip systems in plagioclase (Ji & Mainprice, 1990) and a high-temperature prism <c> slip in quartz.

Úhrov peridotite body shows superposition of two families of LPOs with respect to the geographic coordinates. The family I is characterized by common orientation of (010) planes and [001] axes of all minerals that defines B-type of LPO and a steep NW–SE-striking foliation bearing sub-vertical lineation (Fig. 8; Table 1). The family II shows strong preferred orientation of olivine (010) planes and distribution of [100] and [001] directions typical for axial (010) (AG type) of LPO (Fig. 8; Table 1). This is consistent with NE–SW trending steep foliation and weak, unstable lineation. Small population of pyroxene grains of the family I orientation can be still observed within the family II LPOs (Fig. 8).

	LPO foliation	LPO lineation	LS index	Olivine fabric
Doubrava peridotite				
Peridotite				
8-05-v3	9/87	78/62	x	(010)[001]
8-05-v8	196/67	212/61	x	(010)[001]
8-07-c	344/75	71/74	x	?
8-05-v11	19/80	291/45	x	axial (010)
Pyroxenite				
06-4b	148/84	78/80	0,45	(010)[001]
8-05-v2	311/88	344/85	0,73	x
8-05-v9	162/68	142/66	0,61	x
8-2a	151/66	147/61	0,32	x
8-3a	344/70	26/65	0,43	x
eclogite				
8-05-n	35/72	120/1	0,42	x
8-06-ec	260/89	200/83	0,38	x
Úhrov peridotite				
Peridotite				
khc9	318/77	29/17	x	(010)[100]
khc9a I	148/57	280/50	x	x
khc9a II	241/75	56/1	x	(010)[100]
khc9-b2	61/55	97/49	x	(010)[001]
9-07a	171/62	222/52	x	axial (010)
Spačice eclogite				
Eclogite				
26-05-g	129/78	218/35	0,46	x
26-05-v3 c	172/71	185/66	0,54	x
26-05-v3 f	159/63	111/54	0,33	x

Table 1. *LPOs description of all measured samples; inferred geographic orientations of lineation and foliation, calculated LS indexes and olivine patterns.*

In **Spačice eclogite** (Fig. 9; Table 1), the LPO of clinopyroxene weakens from the coarse-grained to fine grained samples. Maximum density of the strong lineation defined by [001] axes in coarse omphacites decreases, together with LS index, from 0.54 in the coarse-grained to 0.33 in the fine-grained sample. Also position of the lineation changes from steeply plunging towards parallelism of gently plunging fold axes of close folds observed in the field.

6 Discussion

6.1 Relationship between Field Structure and LPO

Detailed field observations carried out in the Běstvina granulite body revealed low-strain domains surrounded by penetrative mylonitic foliations in S_2. Low-strain domains contain unique rock assemblage of coarse-grained granulites associated with either eclogite or clinopyroxenite and of eclogites enclosed in serpentinized peridotite. Field structural measurements show that coarse-grained, sub-vertical and NE–SW trending foliation S_1 in granulites is concordant with pyroxenite layering within the Doubrava peridotite, the dominant fabric in the Úhrov peridotite, as well as with axial planes of tightly folded Spačice eclogite.

The measured LPO of the main rock-forming minerals in the Doubrava peridotite revealed dominant activity of (010)[001] slip system in olivine. The LPO established E–W trending and steeply dipping foliation, which is discordant to the S_1 foliation developed in granulites with clinopyroxenites, and might be interpreted as the original mantle fabric S_0. The LPOs measured in clinopyroxenites as well as coarse-grained granulites, show both foliations S_1 and stretching lineation L_1 to be sub-vertical. Systematic misorientation between steep clinopyroxenite layering measured in the field and foliation determined from the clinopyroxene LPO is very small and close to sampling error, but it may suggest some divergence between origin of layering by magma percolation and superimposed deformation. Eclogite bodies within the Doubrava peridotite show the S type of clinopyroxene LPO with strongly developed foliations being close to the S_0 fabric defined in peridotites (Fig. 7).

In the Úhrov peridotite, LPO data show fabric close to the S_0 determined in the Doubrava peridotite (LPO with the family I grains) as well as NE–SW-striking, sub-vertical fabric that corresponds to the S_1 foliations. The [001] slip direction of all minerals defines steeply plunging stretching lineation on the S_0 foliation, while S_1 is strongly planar fabric with weak unstable lineation. This indicates a reworking of the S_0 fabric bearing a sub-vertical stretching lineation and oblate strain pattern during development of the S_1 fabric. The reworking is attributed to the lack of macroscopic clinopyroxenite layering that could otherwise preferentially localize deformation, leaving coarse-grained peridotite undeformed, as it is the case in the Doubrava peridotite body.

In Spačice eclogite, clinopyroxene LPOs show evolution from LS-type fabric in the coarse-grained to S-type fabric in the fine-grained microstructure. Foliations in both microstructural types are parallel to limbs of upright, close-to-isoclinal folds, the axial plane of which is parallel to the S_1 fabric (Fig. 9b). The stretching lineation defined by a maximum in the distribution of [001] axes rotates from a sub-vertical in the coarse-grained microstructure to a gently plunging, oriented parallel to fold hinge, in the fine-grained microstructure. Microstructural stratification resulting from grain size reduction is attributed to dynamic recrystallization during folding and development of the S_1 fabric in bulk oblate strain.

In all studied mantle-rock bodies, we have documented deformational fabric concordant with relic S_1 granulite fabric. It is the youngest fabric in the mantle rocks because it crosscut or reworked other observed fabrics. Therefore, we can assume that mantle rocks in the Běstvina Formation shared part of their Variscan tectonic history with granulites and granulite gneisses (Synek & Oliveriová, 1993).

6.2 Origin of (001) Slip in Olivine

The latice preferred orientation data show that sub-vertical stretching lineation, inferred from preferred orientation of [001] axes in both pyroxenes, is usually associated with slip along [001]. The activity of the (010)[001] slip system has been variably attributed to (1) presence of mylonites that accommodate low-temperature and high-stress deformation associated with an emplacement of peridotite slices into the crust (e.g. Boudier & Coleman, 1981), (2) pressure increases as confirmed theoretically (Durinck et al., 2005) and experimentally (Mainprice et al., 2005, Jung et al., 2009), (3) hydration (B-type fabric of Jung & Karato, 2001).

In spite of strong serpentinization, the reconstructed peridotite microstructure is not consistent with a high-strain mylonite. At a depth of ~100 km (3.5 GPa), the water content of olivine in equilibrium with basaltic melt (H2O ~ 6 wt. %) would be similar to that estimated for olivine in the MORB source (Hirth & Kohlstedt, 1996). This suggests that the melting process in arc regions may determine the water content of nominally anhydrous phases in the asthenosphere. Thus, the transport of water from the slab into the mantle wedge can continually replenish the water budget in the upper mantle (Hirth & Kohlstedt, 2003). The presence of water and/or high-pressure conditions in the S0 fabric could be a relevant explanation for the development of the olivine B-type fabric. If true, this would indicate an origin of the studied peridotites in a mantle wedge underlying an active magmatic arc (e.g. Kneller et al., 2005).

6.3 Origin of Fabrics and Strain Coupling vs. Tectonic Models

The S_0 fabrics in both Doubrava and Úhrov peridotites as well as the Spačice eclogite correspond to the oldest fabric in studied rocks. Based on previous petrological studies, mainly of spinel inclusions in garnet and prograde zoning of garnet (Medaris et al., 2006a; Faryad, 2009), the fabric is very likely associated with a pressure increase up to either ~4.5 GPa in peridotites or ~3.4 GPa in the eclogite at peak temperatures of ~1,000 °C and ~900 °C, respectively (Faryad, 2009) (Fig. 10). The current LPO study demonstrates that S_0 fabrics in peridotite are linked to B-type LPO of olivine developed at high pressure and/or in the presence of intracrystalline water. These data indicate that the S_0 fabric and prograde metamorphism might develop in the mantle wedge during a flow triggered by subduction of the oceanic lithosphere (Fig. 11). This is in agreement with conclusions of Medaris et al. (2005), even though their tectonic model of the Moldanubian domain being subducted westward below the Teplá-Barrandian cannot be accepted. Crustal rocks of the Moldanubian domain did not undergo prograde HP–LT metamorphism that characterizes subduction geothermal gradient, unlike the Saxothuringian domain further to the west (e.g., Schmädicke & Evans,

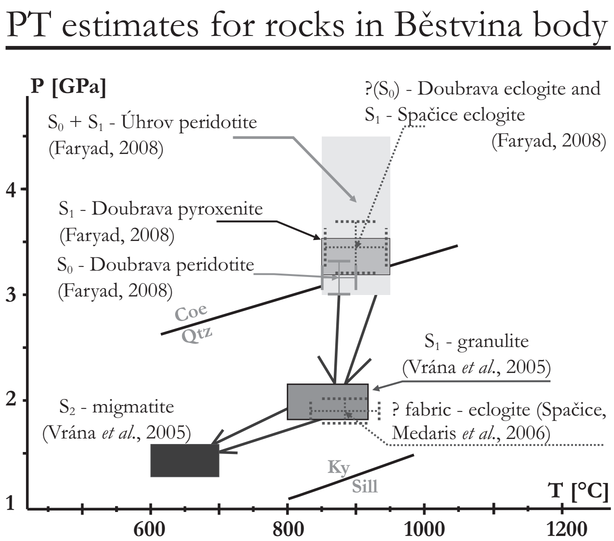

Fig. 10. *A review of calculated peak P-T conditions for the studied rocks with assigned deformation fabrics.*

1997; Konopásek & Schulmann, 2005; Schulmann et al., 2009). It is therefore more likely that the mantle wedge flow and prograde metamorphism occurred above and eastward of the subducted Saxothuringian Ocean (Fig. 11) (O'Brien, 2000; Schulmann et al., 2009). Such a tectonic setting, however, would require an exhumation path for mantle rocks different from that returning along the subduction channel (Schmädicke & Evans, 1997).

In general, the S_1 fabric may correspond to remnants of regionally developed sub-vertical foliation in the orogenic root thickened to approximately 70 km (Schulmann et al., 2005; Tajčmanová et al., 2006; Franěk et al., 2006) in accord with their coarse-grained nature, sub-vertical orientation, and peak P-T conditions of 800–920 °C and 1.8–2.2 GPa (Medaris et al., 1995; Vrána et al., 2005). Thickening of the orogenic root in the Bohemian Massif has been dated between 360 and 345 Ma (Janoušek & Holub, 2007) coeval to the upper crustal intrusion of the magmatic arc (Central Bohemian Plutonic Complex; e.g. Holub et al., 1997; Janoušek et al., 2000; Janoušek et al. 2004b) The intrusions occurred within dextral transpression along the NE–SW-striking sub-vertical foliations (Žák et al., 2005a; Janoušek et al., submitted). Detailed AMS study of the large, c. 354 Ma old Sázava Pluton that belongs to the Central Bohemian Plutonic Complex has shown superposition of regional tectonic strain during transpression on emplacement-related intrusive strain, whereby outer solidified and more rigid NE–SW-striking, sub-vertical edges of the pluton enabled preservation of older, steep stretching in its interior (Žák et al., 2005b).

Common orientations of the NE–SW-striking, sub-vertical S_1 fabric within several isolated low-strain domains suggest that they did not rotate significantly during development of the S_2 fabric. This is consistent with moderate to steeply dipping foliation bearing weak or no stretching lineations as well as rarely preserved symmetric folds that rework the S_1 fabric. Therefore, the strike of the coarse-grained, sub-vertical S_1 foliations in granulites could have regional importance and be correlated with foliations in surrounding tectonic units, namely Central Bohemian Plutonic Complex.

Geochemical analyses of the clinopyroxenites within the Doubrava peridotite indicate that they correspond to a product of reaction between transient basaltic melt and the peridotites, with some crystal accumulation (Machek et al., 2007). Fabrics measured in this work in clinopyroxenite layers yielded a finite-strain ellipsoid that corresponds to emplacement-related intrusive strain recorded in the arc (Sázava Pluton). We suggest that these data may be interpreted in terms of a link between tectonic and magmatic processes spanning the whole lithosphere. In this scenario, basic melt percolation from the mantle wedge overlying the subduction zone, through the thickened crust to the magmatic arc, was responsible for the formation of a NE–SW-striking, sub-vertical zone of localized weakness (Fig. 11). This hypothesis resembles the lithospheric-scale, three-dimensional model of a transpressional arc system, in which the synergy of tectonic and magmatic processes forms a positive feedback loop, which facilitates the upward melt movement (De Saint-Blanquat et al., 1998).

Such a model would link structural, petrological, and geochemical data from the Bohemian Massif, bridging the gap between equilibration conditions of peridotites and eclogites on the one hand and granulites on the other. In this context, the lithological heterogeneity developed due to melt percolation in the mantle wedge represents a key prerequisite for a viscosity partitioning and easy vertical shearing along clinopyroxenite layers. Hence, the whole lithospheric zone of localized weakness might have represented an important pathway for emplacement of deep-seated mantle rocks into the granulitized base of the orogenic root.

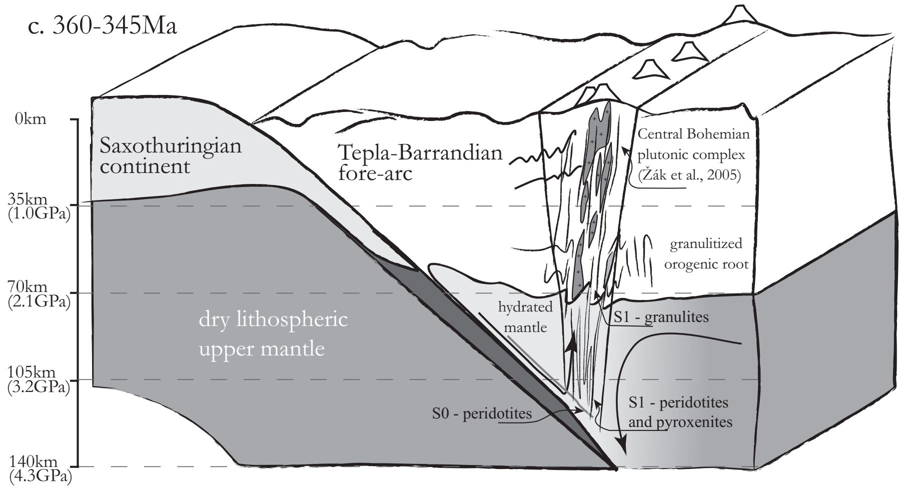

Fig. 11. *A lithospheric-scale, three-dimensional model of a transpressional arc system for the Bohemian Massif, modified from De Saint-Blanquat et al. (1998). The tectonic and magmatic processes are linked, facilitating the upward movement of melt. Arrows indicate positions corresponding to the P-T conditions of equilibration for the studied rocks. Rheological heterogeneity in the mantle wedge due to the development of vertical clinopyroxenite layering caused strain coupling between granulites and clinopyroxenites and emplacement of upper-mantle rocks to the granulitized lower crust.*

The mechanical coupling between the lower crust and upper lithospheric mantle is clearly recorded in granulites and clinopyroxenites bearing a coarse-grained, high-temperature microstructure (Fig. 7). Strain coupling between the upper mantle and the lower crust in the Bohemian Massif has not been expected either in tectonic models based on detailed field structural analysis (e.g. Schulmann et al., 2005) or in models derived from anisotropy of seismic-wave velocities (e.g. Babuška & Plomerová, 2006). The reason for the latter can be seen in the fact that seismic methods have a resolution too low for identification of localized, high-strain zones. On the small scale, however, lithological heterogeneity in the mantle wedge caused by melt percolation would be a model feasible for facilitating strain partitioning and coupling with crustal rocks.

7 Conclusions

The present work revealed two internal strain fabrics in serpentinized peridotites and eclogites in the Kutná Hora Crystalline Complex (the Moldanubian domain of the Bohemian Massif). The oldest fabric, $S_{0,}$ is restricted to the Doubrava and Úhrov peridotites and is represented by sub-vertical, WNW–ESE-striking foliations and sub-vertical lineations. It is associated with coarse-grained microstructure and the B type of olivine LPO. The S_1 fabric is homogeneously developed in surrounding coarse-grained granulites and is characterized by sub-vertical, NE–SW-striking foliations. In peridotites, reworking of the S_0 fabric depends on the presence of macroscopic clinopyroxenite layering. In Doubrava peridotite that is rich in clinopyroxenite layers the S_0 fabric is preserved, while in the Úhrov peridotite the S_0 is reworked into the S_1 fabric. Spačice eclogite is not associated with peridotite and shows the S_0 fabric that was dynamically recrystallized during folding with the axial planes being parallel to the S_1 foliation.

The position of the studied rocks close to the Late Devonian–Early Carboniferous arc, published P-T estimates and geochemical data, and the new fabric analysis document a link between tectonic and magmatic processes spanning the whole Variscan lithosphere. This connection could be attributed to regional, stress-controlled, melt percolation from the Saxothuringian subduction zone through mantle wedge (clinopyroxenites) to the thickened lower crust (granulites) and magmatic arc. The melt percolation resulted in the formation of a NE–SW-striking, sub-vertical zone of localized weakness. Newly developed rheological stratification triggered easy vertical shearing along the clinopyroxenite layers. It was responsible for mechanical coupling between mantle and lower crust that led to the emplacement of mantle wedge fragments into the granulitized lower crust.

Acknowledgements

We are indebted to Shah Wali Faryad (Charles University in Prague) for helpful discussions and revision of the text. We also thank to two anonymous reviewers for their constructive revisions and Larissa Dobrzhinetskaya for careful editorial handling. This work was supported by the Grant Agency of the Czech Republic (GAČR) No. 205/06/0688 and No. 205/09/0539, by the Research Intent of the Geophysical Institute, Academy of Sciences of the Czech Republic, No. AV0Z30120515 and research project MSM0021620855.

References

- *Altherr, R. & Kalt, A., 1996. Metamorphic evolution of ultrahigh-pressure garnet peridotites from the variscan Vosges mts. (France). Chemical Geology, 134, 1-3, 27-47. Babuška, V. & Plomerová, J. 2006. European mantle lithosphere assembled from rigid microplates with inherited seismic anisotropy. Physics of the Earth and Planetary Interiors, 158, 2–4, 264–280.*
- *Barruol, G., Helffrich, G., Vauchez, A., 1997. Shear wave splitting around the northern Atlantic: frozen Pangaean lithospheric anisotropy? Tectonophysics, 279, 1–4, 135–148.*
- *Bascou, J., Tommasi, A. & Mainprice, D. 2002. Plastic deformation and development of clinopyroxene lattice preferred orientations in eclogites. Journal of Structural Geology, 24, 8, 1357–1368.*
- *Ben Ismaïl, W. & Mainprice, D. 1998. An olivine fabric database: an overview of upper mantle fabrics and seismic anisotropy. Tectonophysics, 296, 1–2, 145–157.*
- *Blanquat, M. D. S., Tikoff, B., Teyssier, C. & Vigneresse, J. L. 1998. Transpressional kinematics and magmatic arcs. In: Continental Transpressional and Transtensional Tectonics, Special Publication 135 (eds Holdsworth, R. E., Strachan, R. A. & Dewey, J. F.), pp. 327–340. Geological Society, London.*
- *Boudier, F. & Coleman, R. G. 1981. Cross-section through the peridotite in the Samail Ophiolite, southeastern Oman Mountains. Journal of Geophysical Research, 86, NB4, 2573–2592.*
- *Bystricky, M., Kunze, K., Burlini, L. & Burg, J. P. 2000. High shear strain of olivine aggregates: rheological and seismic consequences. Science, 290, 5496, 1564–1567.*
- *Chopra, P. N. & Paterson, M. S. 1984. The role of water in the deformation of dunite. Journal of Geophysical Research, 89, NB9, 7861–7876.*

- *Dallmeyer, R.D., Franke, W. & Weber, K. (eds.) 1995. Pre-Permian geology of Central and Eastern Europe, Springer, Berlin.*
- *Dudek, A. 1980. The crystalline basement block of the Outer Carpathians in Moravia. Rozpravy Československé Akademie Věd, 90, 8, 1–85.*
- *Durinck, J., Legris, A. & Cordier, P. 2005. Pressure sensitivity of olivine slip systems: first-principle calculations of generalised stacking faults. Physics and Chemistry of Minerals, 32, 8–9, 646–654.*
- *Etheridge, M. A. 1975. Deformation and recrystallization of orthopyroxene from Giles Complex, Central Australia. Tectonophysics, 25, 1–2, 87–114.*
- *Faryad, S. W. 2009. The Kutná Hora Complex (Moldanubian zone, Bohemian Massif): a composite of crustal and mantle rocks subducted to HP/UHP conditions. Lithos, 109, 193–208.*
- *Franěk, J., Schulmann, K. & Lexa, O., 2006. Kinematic and rheological model of exhumation of high pressure granulites in the Variscan orogenic root: example of the Blanský les granulite, Bohemian Massif, Czech Republic. Mineralogy And Petrology, 86, 3-4, 253-276.*
- *Franke, W. 2000. The mid-European segment of the Variscides: tectonostratigraphic units, terrane boundaries and plate tectonic evolution. In: Orogenic Processes: Quantification and Modelling in the Variscan Belt, Special Publication 179 (eds Franke, W., Haak, V., Oncken, O., Tanner, D.), pp. 35–61. Geological Society, London.*
- *Godard, G. & von Roermund, H. L. M. 1995. Deformation-induced clinopyroxene fabrics from eclogites. Journal of Structural Geology, 17, 10, 1425–1443.*
- *Grocott, J., McCaffrey, K.J.W., Taylor, G.K., Tikoff, B., 2004. Vertical coupling and decoupling in the lithosphere. In: Vertical Coupling and Decoupling in the Lithosphere, Special Publication 227 (eds Grocott, J., McCaffrey, K.J.W., Taylor, G. B. and Tikoff B.), pp. 1–8. Geological Society, London.*
- *Hirth, G. & Kohlstedt, D. L., 1996. Water in the oceanic upper mantle: Implications for rheology, melt extraction and the evolution of the lithosphere. Earth and Planetary Science Letters, 144, 1-2, 93-108.*
- *Hirth, G., and Kohlstedt, D. 2003. Rheology of the upper mantle and the mantle wedge: A view from the experimentalists, In: Inside the subduction factory, American Geophysical Union, Geophysical Monograph 138 (ed. Eiler, J.), pp. 88–105. AGU, Washington, D.C.*
- *Helmstaedt, H., Anderson, O.L., Gavasci, A.T. 1972. Petrofabric studies of eclogite, spinel–websterite, and spinel–lherzolite xenoliths from kimberlite-bearing breccia pipes in southeastern Utah and northeastern Arizona. Journal of Geophysical Research, 77, 4350–4365.*
- *Holub, F. V., Cocherie, A. & Rossi, P. 1997. Radiometric dating of granitic rocks from the Central Bohemian Plutonic Complex (Czech Republic): constraints on the chronology of thermal and tectonic events along the Moldanubian-Barrandian boundary. Comptes Rendus Academie des Sciences Serie II: Sciences de la Terre et des Planetes, 325, 1, 19–26.*
- *Holub, F. V. & Munchi, R. L. 1984. Subsolidus reaction rims between olivine and calcic plagioclase in the Svatý Kříž massif, Eastern Bohemia. Krystalinikum, 17, 47–58.*
- *Janoušek, V. & Holub, F.V. 2007. The causal link between HP-HT metamorphism and ultrapotassic magmatism in collisional orogens: case study from the Moldanubian Zone of the Bohemian Massif. Proceedings of the Geologists’ Association, 118, 75–86.*

- *Janoušek, V., Bowes, D. R., Rogers, G., Farrow, C. M. & Jelínek, E. 2000. Modelling diverse processes in the petrogenesis of a composite batholith: the Central Bohemian Pluton, Central European Hercynides. Journal of Petrology, 41, 4, 511–543.*

- *Janoušek, V., Braithwaite, C. J. R., Bowes, D. R. & Gerdes, A. 2004b. Magma-mixing in the genesis of Hercynian calc–alkaline granitoids: an integrated petrographic and geochemical study of the Sázava intrusion, Central Bohemian Pluton, Czech Republic. Lithos, 78: 67–99.*

- *Janoušek, V., Finger, F., Roberts, M. P., Frýda, J., Pin, C. & Dolejš, D. 2004a. Deciphering petrogenesis of deeply buried granites: whole–rock geochemical constraints on the origin of largely undepleted felsic granulites from the Moldanubian Zone of the Bohemian Massif. Transactions of the Royal Society of Edinburgh – Earth Sciences, 95, 141–159.*

- *Janoušek, V., Wiegand, B., Žák, J. & Erban, V. Timing the onset of crustal exhumation in the core of the Bohemian Massif: new SHRIMP U–Pb zircon ages from the high–K calc–alkaline granodiorites of the Blatná suite, Central Bohemian Plutonic Complex. Journal of the Geological Society, London (Submitted).*

- *Ji, S. C. & Mainprice, D. 1990. Recrystallization and fabric development in plagioclase. Journal of Geology, 98, 1, 65–79.*

- *Jung, H. & Karato, S. 2001. Water-induced fabric transitions in olivine. Science, 293, 5534, 1460–1463.*

- *Jung, H., Mo, W., Green, H. W. 2009. Upper mantle seismic anisotropy resulting from pressure-induced slip transition in olivine. Nature Geoscience, 2, 73–77.*

- *Katayama, I., Jung, H. & Karato, S. I. 2004. New type of olivine fabric from deformation experiments at modest water content and low stress. Geology, 32, 12, 1045–1048.*

- *Kneller, E. A., van Keken, P. E., Karato, S. & Park, J., 2005. B-type olivine fabric in the mantle wedge: Insights from high-resolution non-Newtonian subduction zone models. Earth and Planetary Science Letters, 237, 3-4, 781-797.*

- *Kneller, E. A., van Keken, P. E., Katayama, I. & Karato, S. 2007. Stress, strain, and B-type olivine fabric in the fore-arc mantle: sensitivity tests using high-resolution steady-state subduction zone models. Journal of Geophysical Research-Solid Earth, 112, B4, B004406.*

- *Konopásek, J. & Schulmann, K. 2005. Contrasting Early Carboniferous field geotherms: evidence for accretion of a thickened orogenic root and subducted Saxothuringian crust (Central European Variscides). Journal of the Geological Society London, 162, 3, 463–470.*

- *Košler, J., Aftalion, M. & Bowes, D. R. 1993. Mid-late Devonian plutonic activity in the Bohemian Massif: U-Pb zircon isotopic evidence from the Staré Sedlo and Mirotice gneiss complexes, Czech Republic. Neues Jahrbuch für Mineralogie, Monatshefte, 9, 417– 431.*

- *Lexa, O., Štípská, P., Schulmann, K., Baratoux, L. & Kröner, A., 2005. Contrasting textural record of two distinct metamorphic events of similar P-T conditions and different durations. Journal of Metamorphic Geology, 23, 8, 649–666.*

- *Mackwell, S. J., Kohlstedt, D. L. & Paterson, M. S. 1985. The role of water in the deformation of olivine single–crystals. Journal of Geophysical Research–Solid Earth and Planets, 90, NB13, 1319–1333.*

- *Machek M., Ulrich S., Janoušek V., Faryad S.W. 2007. Mantle wedge flow and emplacement to a granulitized crust – natural example from the Doubrava upper mantle rock in the Bohemian Massif. 16th Meeting of DRT conference, Milan, Italy. Abstract volume DRT 2007, Rediconti della Societa Geologica Italiana, 5, 139–140.*

- *Mainprice, D. 2005. The Unicef careware petrophysical software package. ftp://www.gm.univ-montp2.fr/mainprice//CareWare_Unicef_Programs/*

- *Mainprice, D., Tommasi, A., Couvy, H., Cordier, P. & Frost, D. J. 2005. Pressure sensitivity of olivine slip systems and seismic anisotropy of Earth's upper mantle. Nature 433, 7027, 731–733.*

- *Mauler, A., Godard, G. & Kunze, K. 2001. Crystallographic fabrics of omphacite, rutile and quartz in Vende'e eclogites (Armorican Massif, France). Consequences for deformation mechanisms and regimes. Tectonophysics, 342, 1–2, 81–112.*

- *Medaris, L. G., Beard, B. L. & Jelínek, E. 2006a. Mantle-derived, UHP garnet pyroxenite and eclogite in the Moldanubian Gföhl nappe, Bohemian Massif: a geochemical review, new P–T determinations, and tectonic interpretation. International Geology Review, 48, 9, 765–777.*

- *Medaris, L. G., Beard, B. L., Johnson, C. M., Valley, J. W., Spicuzza, M. J., Jelínek, E. & Mísař, Z. 1995. Garnet pyroxenite and eclogite in the Bohemian Massif—geochemical evidence for Variscan recycling of subducted lithosphere. Geologische Rundschau, 84, 3, 489–505.*

- *Medaris, L. G., Ghent, E. D., Wang, H. F., Fournelle, J. H. & Jelínek, E. 2006b. The Spačice eclogite: constraints on the P-T-t history of the Gföhl granulite terrane, Moldanubian Zone, Bohemian Massif. Mineralogy and Petrology, 86, 3–4, 203–220.*

- *Medaris, G., Wang, H., Jelínek, E., Mihaljevič, M. & Jakeš, P. 2005. Characteristics and origins of diverse Variscan peridotites in the Gföhl Nappe, Bohemian Massif, Czech Republic. Lithos, 82, 1–2, 1–23.*

- *Medaris, L. G., Wang, H. F., Mísař, Z. & Jelínek, E. 1990. Thermobarometry, Diffusion modeling and cooling rates of crustal garnet peridotites—2 examples from the Moldanubian Zone of the Bohemian Massif. Lithos, 25, 1–3, 189–202.*

- *Mísař, Z., Dudek, A., Havlena, V., Weiss, J., 1983. Geologie ČSSR: I. Český masiv. Státní Pedagogické Nakladatelství, Praha, 333 pp. In Czech.*

- *Molnar, P. 1992. Brace-Goetze strength-profiles, the partitioning of strike slip and thrust faulting at zones of oblique convergence, and stress heat flow paradox of the San Andreas Fault. In: Fault Mechanics and Transport Properties of Rocks (eds Evans, B. & Wong, T.F.), Academic Press, London.*

- *Munchi, R. L. 1978. Metabasites and associated rocks in Ronov–Moravany area, Eastern Bohemia. Acta Universitatis Carolinae – Geologica, 3–4, 293–305.*

- *Munchi, R. L. 1981. Petrology of gabbro-amphibolite complex, Ronov–Moravany area, Eastern Bohemia. Acta Universitatis Carolinae – Geologica, 1, 19–33.*

- *O'Brien, P. J., 2000. The fundamental Variscan problem: high-temperature metamorphism at different depths and high-pressure metamorphism at different temperatures. In: Orogenic Processes: Quantification and Modelling in the Variscan Belt, Special Publication 179 (eds Franke, W., Haak, V., Oncken, O., Tanner, D.), pp. 369–386. Geological Society, London.*

- *Pouba, Z., Fiala, J. & Paděra, K. 1987. Granulite body near Běstvina in Železné hory mountains. Časopis pro Mineralogii a Geologii, 32, 1, 73–78. In Czech. Ross, J. V. & Nielsen, K. C. 1978. High-temperature flow of wet polycrystalline enstatite. Tectonophysics, 44, 1–4, 233–261.*

- *Sawaguchi, T. & Ishii, K. 2003. Three-dimensional numerical modeling of lattice—and shape-preferred orientation of orthopyroxene porphyroclasts in peridotites. Journal of Structural Geology, 25, 9, 1425–1444.*

- *Schulmann, K., Konopásek, J., Janoušek, V., Lexa O., Lardeaux, J-M., Edel, J-B., Štípská, P. & Ulrich, S., 2009. An Andean type Palaeozoic convergence in the Bohemian Massif, Comptes Rendus Geoscience, 341, 266–286.*

- *Schulmann, K., Kröner, A., Hegner, E., Wendt, I., Konopásek, J., Lexa, O. & Štípská, P. 2005. Chronological constraints on the pre–orogenic history, burial and exhumation of deep-seated rocks along the eastern margin of the Variscan Orogen, Bohemian Massif, Czech Republic. American Journal of Science, 305, 5, 407–448.*

- *Schulmann, K., Lexa, O., Štípská, P., Racek, M., Tajčmanová, L., Konopásek, J., Edel, J-B., Peschler, A., Lehmann, J. 2008. Vertical extrusion and horizontal channel flow of orogenic lower crust: key exhumation mechanisms in large hot orogens? Journal of Metamorphic Geology, 26, 2, 273–297.*

- *Schmädicke, E. & Evans, B. W., 1997. Garnet-bearing ultramafic rocks from the Erzgebirge, and their relation to other settings in the Bohemian Massif. Contributions to Mineralogy and Petrology, 127, 1-2, 57-74.*

- *Suess, F. E. 1926. Intrusionstektonik und Wandertektonik im variszischen Grundgebirge. Bornträger, Berlin.*

- *Synek, J. & Oliveriová, D. 1993. Terrane character of the northeast margin of the Moldanubian Zone—the Kutná Hora Crystalline Complex, Bohemian Massif. Geologische Rundschau, 82, 3, 566–582.*

- *Tait, J. A., Bachtadse, V. & Soffel, H. 1996. Eastern Variscan fold belt: paleomagnetic evidence for oroclinal bending. Geology, 24, 10, 871–874*

- *Tajčmanová, L., Konopásek, J. & Schulmann, K., 2006. Thermal evolution of the orogenic lower crust during exhumation within a thickened Moldanubian root of the Variscan belt of Central Europe. Journal of Metamorphic Geology, 24, 2, 119-134.*

- *Timmerman, M. J., 2008. Palaeozoic magmatism. In: The Geology of Central Europe. Volume 1: Precambrian and Palaeozoic (ed. McCann, T.), pp. 665–748. Geological Society, London.*

- *Tikoff, B., Russo, R., Teyssier, C., Tommasi, A., 2004. Mantle-driven deformation of orogenic zones and clutch tectonics. In: Vertical Coupling and Decoupling in the Lithosphere, Special Publication 227 (eds Grocott, J., McCaffrey, K.J.W., Taylor, G. B. and Tikoff B.), pp. 41–64. Geological Society, London.*

- *Tommasi, A., Mainprice, D., Canova, G. & Chastel, Y. 2000. Viscoplastic self–consistent and equilibrium-based modeling of olivine lattice preferred orientations: implications for the upper mantle seismic anisotropy. Journal of Geophysical Research—Solid Earth, 105, B4, 7893–7908.*

- *Tommasi, A., Tikoff, B. & Vauchez, A. 1999. Upper mantle tectonics: three-dimensional deformation, olivine crystallographic fabrics and seismic properties. Earth and Planetary Science Letters, 168, 1–2, 173–186.*

- *Ulrich, S. & Mainprice, D. 2005. Does cation ordering in omphacite influence development of lattice–preferred orientation? Journal of Structural Geology, 27, 3, 419–431.*

- *Vauchez, A., Barruol, G., 1996. Shear-wave splitting in the Appalachians and the Pyrenees: importance of the inherited tectonic fabric of the lithosphere. Physics of the Earth and Planetary Interiors, 95, 3–4, 127–138.*

- *Vigneresse, J.L., Burg, J.P., 2004. Strain-rate-dependent rheology of partially molten rocks In: Vertical Coupling and Decoupling in the Lithosphere, Special Publication 227 (eds Grocott, J., McCaffrey, K.J.W., Taylor, G. B. and Tikoff B.), pp. 327–336. Geological Society, London.*

- *Vrána, S., Štědrá, V. & Fišera, M. 2005. Petrology and geochemistry of the Běstvina granulite body metamorphosed at eclogite facies conditions, Bohemian Massif. Journal of the Czech Geological Society, 50, 3–4, 95–106.*

- *Žák, J., Holub, F. & Verner, K. 2005a. Tectonic evolution of a continental magmatic arc from transpression in the upper crust to exhumation of mid-crustal orogenic root recorded by episodically emplaced plutons: the Central Bohemian Plutonic Complex (Bohemian Massif). International Journal of Earth Sciences, 94, 3, 385–400.*

- *Žák, J., Schulmann, K. & Hrouda, F. 2005b. Multiple magmatic fabrics in the Sázava pluton (Bohemian Massif, Czech Republic): a result of superposition of wrench-dominated regional transpression on final emplacement. Journal of Structural Geology, 27, 5, 805–822.*

- *Zhang, S. Q., Karato, S., Fitz Gerald, J. D., Faul, U. H. & Zhou, Y. 2000. Simple shear deformation of olivine aggregates. Tectonophysics, 316, 1–2, 133–152.*

- *Ziegler, P. A. 1986. Geodynamic model for the Paleozoic crustal consolidation of Western and Central Europe. Tectonophysics, 126, 2–4, 303–328.*

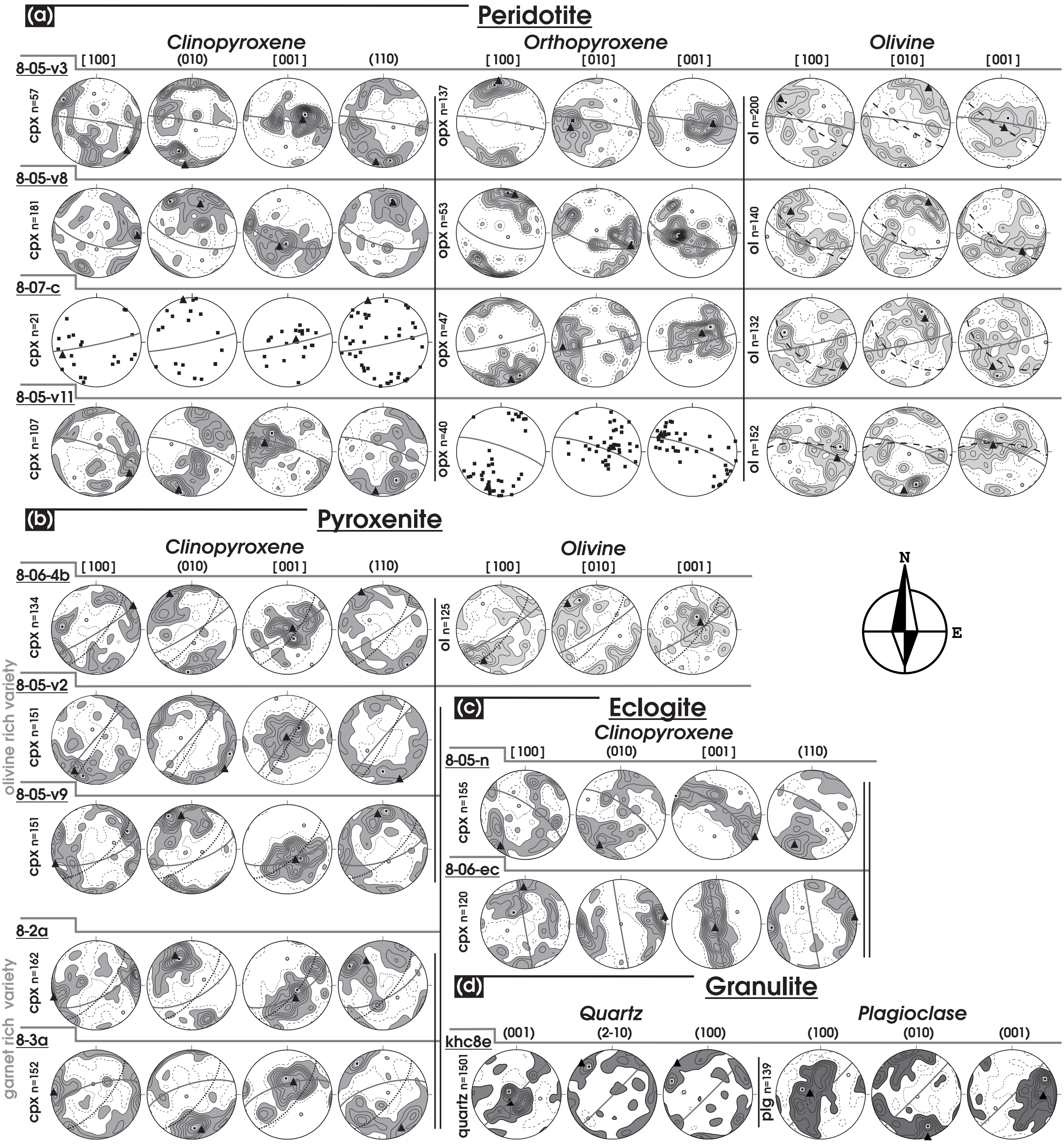

Fig. S1 *Lattice preferred orientations (LPO) of main rock-forming minerals of all samples measured at Doubrava peridotite body (locality 8). Pole figure was constructed, and symbols used, in the same way as in Fig. 6. (a) LPOs of clinopyroxene, olivine, and orthopyroxene in peridotite. (b) LPOs of clinopyroxene and olivine in clinopyroxenite. (c) LPO of clinopyroxene in eclogite. (d) LPOs of quartz and plagioclase in granulite.*